Research Article

Journal of Environmental Nanotechnology

Density Analysis of rGO–Nanodiamond Hybrid Nanofluids Based on Water, Ethylene Glycol and their Mixtures

B. Deepanraj* and L. Syam Sundar

Department of Mechanical Engineering, College of Engineering, Prince Mohammad Bin Fahd University, Al-Khobar, Saudi Arabia

Received: 20.06.2025 Accepted: 10.08.2025 Published: 30.09.2025

*babudeepan@gmail.com

ABSTRACT

This work examines the density of a mixture of reduced graphene oxide–nanodiamond (rGO–ND) nanoparticles dispersed in five different nanofluids. The base fluids considered in this study are water, ethylene glycol, 80:20% W+EG, 60:40% W+EG, and 40:60% W+EG mixtures. In order to prepare the stable hybrid nanofluids, the graphene oxide-nanodiamond hybrid nanoparticles were dispersed in the base fluids. Measurements were performed under different volume loadings ($0 < \phi < 1.0\%$), and different temperatures ($293\ K < T < 333\ K$). An increase in density was observed with increasing volume loadings and temperatures. A maximum density enhancement of 1.1314% was observed for the case of water-based hybrid nanofluids compared to the other nanofluids. Based on the obtained data, non-linear regression equations were proposed.

Keywords: Particle size; Density; Nanoparticles; Hybrid nanofluids.

1. INTRODUCTION

Nanofluids are suspensions of nanoparticles (at least one dimension smaller than 100 nm) in a base fluid with superior thermal, rheological, and wettability properties. They improve heat transfer, lubrication, drug delivery, and better oil recovery. In order to conserve a significant amount of energy, industries need an efficient heat exchange system (Satti *et al.* 2016; Shahrul *et al.* 2014; Yıldırımcan, 2024; Srinivasan *et al.* 2024). In the past few decades, a variety of strategies have been used to achieve high heat transfer efficiency. Previous investigations (Ahuja, 1975) used microstructures, which ran into problems due to clumping. Choi and Eastman, (1995) later introduced fluids with high thermal conductivity known as nanofluids.

Base fluids, such as water, ethylene glycol, propylene glycol, engine oil, and others, often have lower thermal conductivities and are frequently employed in heat exchangers, solar collectors, and other thermal devices. To improve the performance of these devices, high thermal conductivity fluids must replace these fluids. Ag, Al_2O_3, Au, Cu, CuO, Fe_2O_3, Fe_3O_4, MgO, MWCNT, graphene oxide, diamond, SiO_2, TiO_2, ZnO, ZrO_2, are a few examples (Chiam *et al.* 2017; Liu *et al.* 2011; Radkar *et al.* 2019; Elsaid *et al.* 2021). Vallarasu *et al.* (2023) highlighted the practical importance of dispersing nanoparticles into liquid media for catalytic degradation applications, emphasizing their potential for multiple uses.

The utilization of nanofluids in thermal devices was demonstrated by Sundar *et al.* (2012), and Pathipakka and Sivashanmugam, (2010) to increase the rate at which heat is transferred. The majority of prior studies on nanofluids concentrated on their characterization and thermal conductivity; however, in recent years, attention has turned to the viscosity of nanofluids (Sundar *et al.* 2016a). The exact thermal characteristics of nanofluids have not yet been thoroughly confirmed, despite the studies (Hachey *et al.* 2014; Nguyen *et al.* 2008).

Density of nanofluids is very important, because while dispersing the nanoparticles into the base fluids, the base fluid density will increase. This increased density of the nanofluids causes clogging. So, it is necessary to understand the density of the nanofluids. Some of the research works related to the density evaluations are mentioned here. Yadav *et al.* (2021) estimated the density of EG-based Al_2O_3, CuO and CeO_2 nanofluids in the volume concentrations of 0.2%, 0.5%, 0.8%, 1%, and 1.5% in the temperatures range from 20 °C to 80 °C and they developed four different density equations. Jamei *et al.* (2022) considered 501 density data points from various researchers and used multivariate adaptive regression spline (MARS), evolutionary polynomial regression (EPR), gene expression programming (GEP) and multivariate linear regression (MLR) models to predict the density data. They observed that MARS and EPR pattern provided accurate density data compared to other models.

Vajjha *et al.* (2006) observed that ZnO nanofluid deviates larger with the theoretical data. Zhelezny *et al.* (2017) evaluated the density and specific heat of Al_2O_3 nanofluids and observed an increased density with larger particle volume loadings. Montazer *et al.* (2018) measured the density of MWCNT and f-GNP nanofluids at 0.1 vol.% and from 20°C to 40°C and they observed density raise of 0.15% at 0.1% vol. of MWCNT–COOH nanofluid against the base fluid. They also observed the density increase of 0.056% for f-GNP nanofluids. They used response surface method model and predicted the density of MWCNT–COOH and f-GNP nanofluids with an accuracy of 0.012% and 0.009%, respectively.

The aim of the present study is experimentally obtain the density of reduced graphene oxide (rGO)-ND dispersed in water, EG, 80:20%, 60:40%, and 40:60% W+EG (mass) mixture fluids. Data were collected at various temperatures and volume loading.

2. MATERIALS AND METHODS

2.1 Preparation of Hybrid Nanofluids

Reduced graphene oxide nanosheets were synthesized using the Hummers method (Hummers and Offman, 1958). About 5 g of graphite was mixed with 200 mL of H_2SO_4 and 0.025 M of $NaNO_3$. The solution was cooled in an ice bath for 30 minutes. Later, 0.041 moles of $KMnO_4$ were added to the chilled solution. The mixture was treated with 30% (w/w) H_2O_2 for 30 minutes to remove impurities. The solution was washed several times with de-ionized water. The rGO nanosheets were separated by centrifugation and then dried in an oven at 60°C for 12 hours. To introduce –COOH groups onto the rGO surface, the material was washed with HCl for 48 hours. This treatment resulted in a significant yield of functionalized rGO.

Purification of the commercially available nanodiamond (ND)-soot was performed using method described by Sundar *et al.* (2016b). Typically, 10 g of ND-soot was dispersed in a 1:3 molar ratio mixture of sulfuric acid and nitric acid and then stirred for 72 hours. The resulting mixture was then washed several times with DI-water to remove residual acids. This method introduced -COOH groups onto the ND surface and improved the dispersion of ND on rGO.

Reduced graphene oxide and nanodiamond (70:30 wt%) were mixed together in the base fluid. Due to a lack of information on rGO-ND hybrid nanofluids, this ratio was chosen randomly. The density of rGO and ND were found by using the law of mixtures (Eq. 1). The density of nanoparticles and base fluids are given in Table 1.

$$\rho_{(rGO/ND)_p} = \frac{\rho_{rGO} \times W_{rGO} + \rho_{ND} \times W_{ND}}{W_{rGO} + W_{ND}} \quad \ldots (1)$$

Table 1. Densities of substances

Substance		ρ, kg/m^3
Nanoparticles	ND	3100
	rGO	1910
	rGO-ND (70:30 wt%)	2267
Fluids	Water	998
	80:20%	1029.72
	60:40%	1059.68
	40:60%	1086.27
	Ethylene glycol	1121.23

For nanofluid preparation, the rGO-ND was mixed with the base fluid. For this analysis, 0.2%, 0.4%, 0.6%, 0.8%, and 1.0 vol % were considered.

$$\phi = \frac{\left[\frac{W_{rGO-ND}}{\rho_{rGO-ND}}\right]}{\left[\frac{W_{rGO-ND}}{\rho_{rGO-ND}}\right] + \left[\frac{W_{bf}}{\rho_{bf}}\right]} \times 100 \quad \ldots (2)$$

Eq. (2) yielded the density of necessary particle volume loadings for rGO-ND nanoparticles, which was then utilized in Eq. (3). Hybrid nanofluids weighing 20 g were prepared and their properties were assessed. Table 2 shows the expected quantity of dry rGO-ND nanoparticles. In a 100 mL beaker, 0.091 g of rGO-ND nanoparticles were introduced to 20 g of water-based hybrid nanofluids. The combination was then sonicated using an ultrasonicator to produce ϕ = 0.2% nanofluid. Similarly, 0.081 g of rGO-ND was added to 20 g of EG-based hybrid nanofluids in a 100 mL beaker to produce ϕ = 0.2% vol. of nanofluid. The same procedure was repeated for the production of nanofluids with different concentrations (0.4%, 0.6%, 0.8%, and 1.0%).

Table 2. Required composition of nanoparticles

Vol. (%)	Nanoparticles (g)				
	Water	80:20% W+EG	60:40% W+EG	40:60% W+EG	EG
0.2%	0.091	0.088	0.085	0.083	0.081
0.4%	0.182	0.176	0.171	0.167	0.162
0.6%	0.274	0.265	0.258	0.251	0.244
0.8%	0.366	0.355	0.345	0.336	0.326
1.0%	0.459	0.444	0.432	0.421	0.408

The dispersion status of the synthesized nanofluids was assessed using a Zetasizer Nano ZS, Malvern, and the results are displayed in Table 3. As the observed zeta potential values is greater than ±30 mV, the synthesized nanofluids are considered stable.

Table 3. Stability values

Vol. (%)	Zeta Potential (mV)				
	Water	80:20% W+EG	60:40% W+EG	40:60% W+EG	EG
0.2	–44	–42	–43	–44	–40
0.4	–43	–40	–41	–41	–41
0.6	–41	–39	–40	–40	–38
0.8	–40	–38	–38	–37	–39
1.0	–39	–37	–36	–38	–38

2.2 Density Measurements

The density of nanofluids was estimated based on the Archimedes principle

$$\rho = m/v \quad \ldots (3)$$

where, ρ is the density (kg/m^3), m is the mass (kg), and v is the volume (m^3).

From Eq. (3), the weight of a known volume of nanofluid was measured using precision Metter Toledo balance. Initially, the density of base fluid was determined by pouring it into a beaker of known volume and measuring its mass. Later, the analysis was extended to different volume concentrations and different base fluids. For each case, 0.2% volume concentration of nanofluid was poured into a beaker of known volume, and its mass was measured using a precision balance. The procedure was repeated for all other nanofluids.

3. RESULTS AND DISCUSSION

3.1 XRD Analysis

Using a Phillips X'PERT PRO X-ray diffractometer and Cu Kα radiation (λ = 1.54 Å), the X-ray diffraction (XRD) patterns of reduced graphene oxide and nanodiamond were independently determined and are presented in Figs. 1(a) and 1(b). These patterns were previously reported in the author's own publication (Sundar, 2024) and are reused here with appropriate citation and permission from the publisher. As observed for rGO, the characteristic (002) and (100) diffraction peaks appeared at 24.5° and 41.31°, respectively. In the instance of ND, the intensity peaks (111), (220), and (311), were recorded at 43.52°, 75.02°, and 91.43°, respectively. The particle size was determined using Debye Scherrer's equation.

$$D = 0.9\lambda / \beta\cos\theta \quad \ldots (4)$$

The 2θ angle of peak (002) for rGO is 23.9° and its β is 0.15 rad. The rGO size was estimated from Eq. (4) and is found to be 56.55 nm. The 2θ angle of peak (111) for ND is 43.45° and its β is 0.85 rad. The ND size was estimated from Eq. (4) and is found to be 10.52 nm.

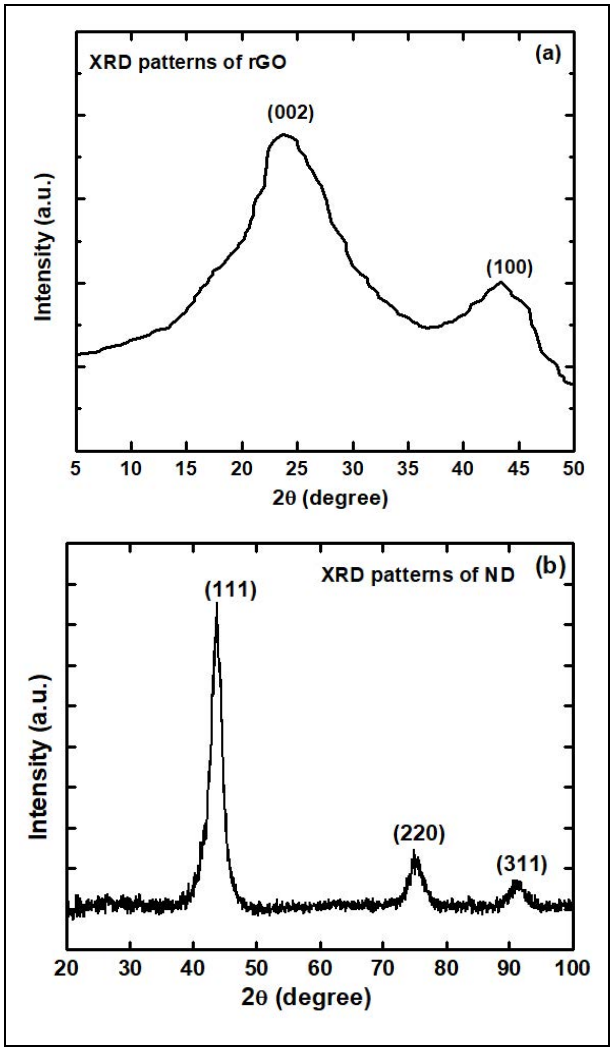


Fig. 1: XRD results: (a) rGO, and (b) nanodiamond (Sundar, 2024)

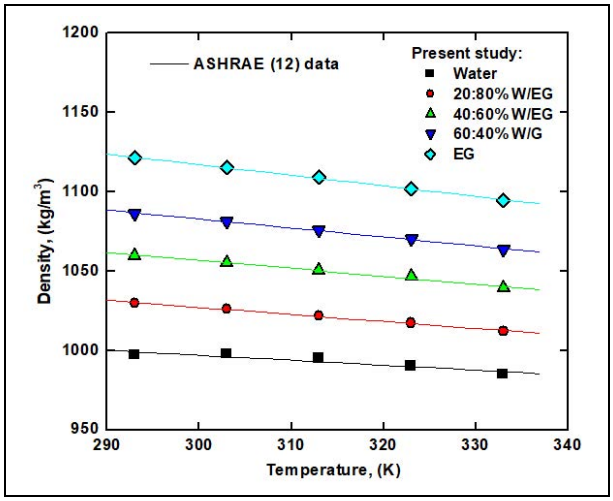


Fig. 2: Base fluid density compared with ASHRAE data

3.2 Density of Nanofluids

Initially, the density of base fluids was measured and the values are provided in Fig. 2. It was observed that the density of the base fluids perfectly matches with the ASHRAE (2005) data. A deviation of 2.12% was noticed.

Since the base fluids exhibited minimal variation in density measurements, the study was extended to hybrid nanofluids at different volume concentrations. For the density analysis, the nanofluids were prepared in water, 80:20, 60:40, 40:60 W+EG (mass %) and EG. The mixture of W+EG is used as engine coolant in countries with subzero temperatures. Density values of water hybrid nanofluids are provided in Fig. 3. The density is seen to increase at higher volumes and decrease with rise of temperatures. Higher increase of density by 1.056% and 1.072% was noticed for ϕ = 1.0% and at a temperature of 293 K and 333 K, over base fluid.

The density of 80:20% W+EG mixture nanofluids is shown in Fig. 4. The density is seen to increase with higher loadings and decrease at higher temperatures. Density reaches 1.06% and 1.09% higher for 1.0 vol% at temperatures of 293 K and 333 K over 80:20 W+EG fluid. Similar trend was seen for density 60:40, 40:60 W+EG and EG nanofluids (Fig. 5, 6 and 7). The density was noticed to increase with the influence of larger particles but decreased with higher temperatures. Density of 60:40% W/EG hybrid nanofluid goes to 1.074% and 1.083% more for 1.0 vol% and at temperature of 293 K and 333 K over base fluid (Fig. 5). Density of 40:60% was 1.064% and 1.097% higher at 1.0% and at temperature of 293 K and 333 K over base fluid (Fig. 6). Density of EG based hybrid nanofluid increased by 1.098% and 1.11% further at 1.0% and at a temperature of 293 K and 333 K against the base fluid (Fig. 7). Table 4 indicates the obtained density data for various nanofluids.

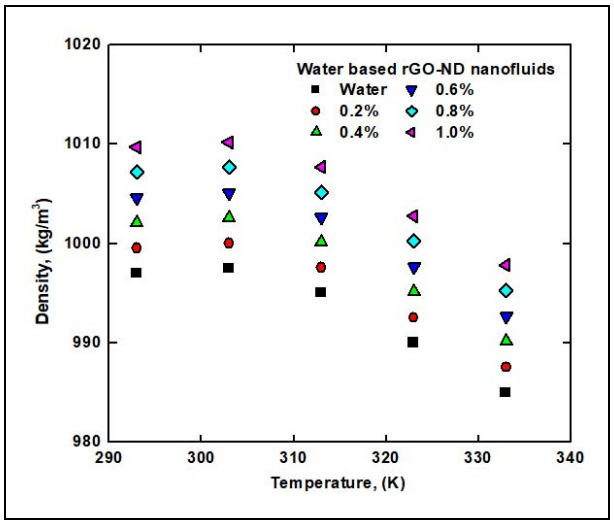


Fig. 3: Density of water-based hybrid nanofluid with respect to temperatures

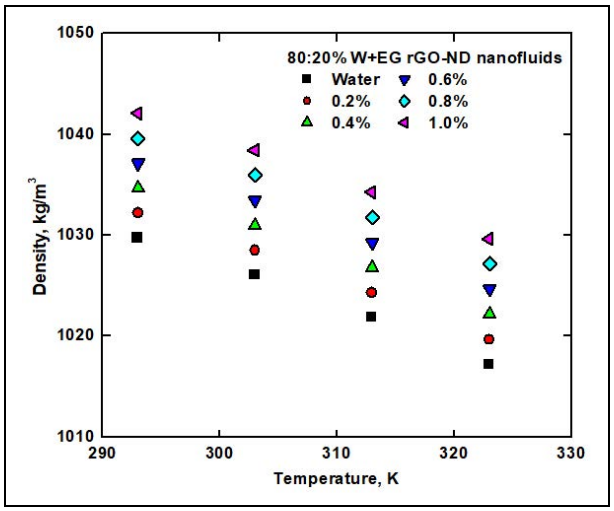


Fig. 4: Density of 80:20% W/EG hybrid nanofluid with respect to temperatures

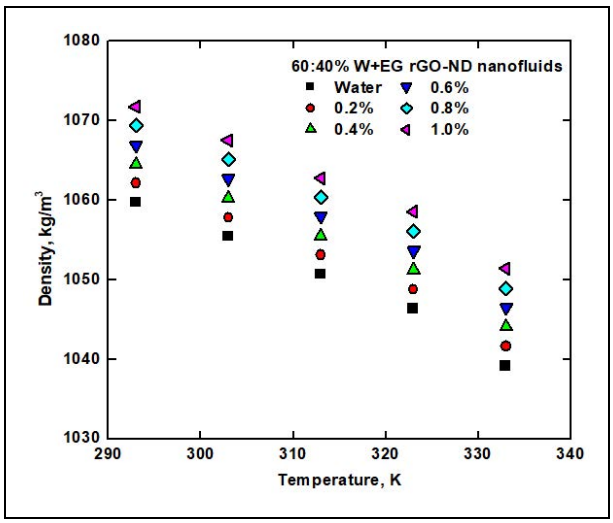


Fig. 5: Density of 60:40% W/EG hybrid nanofluid with respect to temperatures

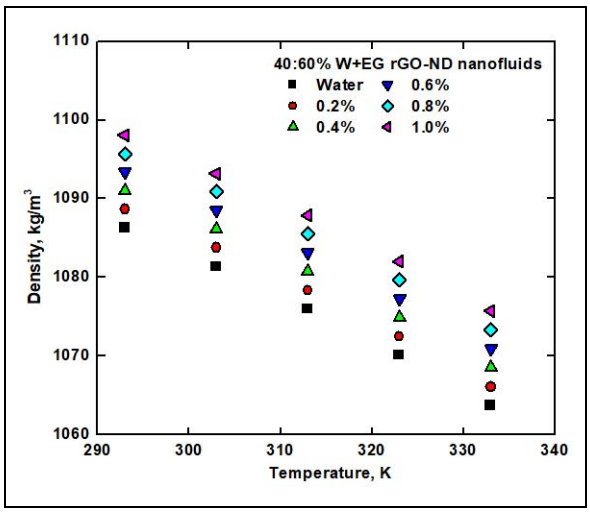


Fig. 6: Density of 40:60% W/EG hybrid nanofluid with respect to temperatures

3.3 Development of Experimental Data

The obtained density of the prepared nanofluids was made into a single regression for easy use of density data at the required temperatures.

Base fluid: water

$$\rho_{nf} = 1091.0089 - 0.3134\,T + 12.7437\phi \quad \ldots (5)$$

Base fluid: 80:20% W+EG

$$\rho_{nf} = 1159.360 - 0.44095T + 12.4571\phi \quad \ldots (6)$$

Base fluid: 60:40% W+EG

$$\rho_{nf} = 1206.5826 - 0.49955T + 12.168\phi \quad \ldots (7)$$

Base fluid: 40:60% W+EG

$$\rho_{nf} = 1251.264 - 0.561667T + 11.918\phi \quad \ldots (8)$$

Base fluid: EG

$$\rho_{nf} = 1315.732 - 0.6624T + 11.586\phi \quad \ldots (9)$$

The range is: $0.0\% < \phi < 1.0\%$, and $293K < T < 333K$

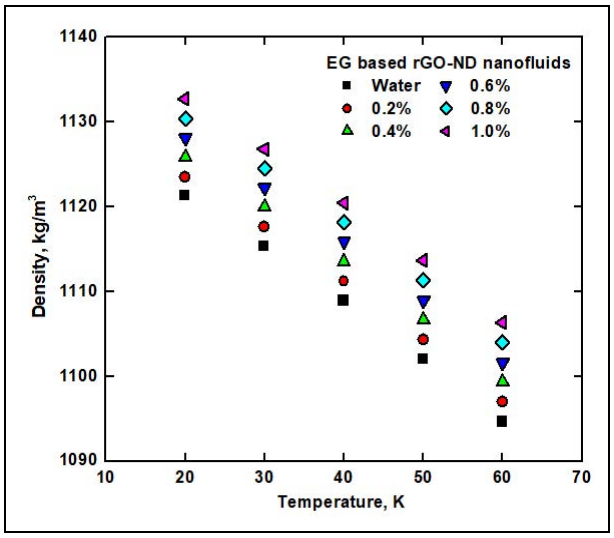


Fig. 7: Density of EG based hybrid nanofluid with respect to temperatures

4. CONCLUSION

The density of water, 80:20%, 60:40%, 40:60% W+EG, and EG-based rGO-ND hybrid nanofluids were experimentally examined in this work. Experimental findings show that the density of hybrid nanofluids increases as particle volume loadings increase and decrease with temperatures that rise above that of the base fluids. While the density is higher for ethylene glycol-based nanofluids, it is lower for DI water nanofluids. These findings inspire other researchers working in the field of nanofluids to determine the viability of the suggested methodology for additional research into the properties of nanofluids.

FUNDING

This research received no specific grant from any funding agency in the public, commercial, or not-for-profit sectors.

CONFLICTS OF INTEREST

The authors declare that there is no conflict of interest.

COPYRIGHT

This article is an open-access article distributed under the terms and conditions of the Creative Commons Attribution (CC BY) license (http://creativecommons.org/licenses/by/4.0/).

REFERENCES

Ahuja, A. S., Augmentation of heat transport in laminar flow of polystyrene suspensions. I. Experiments and results, *J. Appl. Phys*., 46, 3408-3416 (1975). https://doi.org/10.1063/1.322107

ASHRAE, Handbook Fundamentals, American Society of Heating, Refrigerating and Air-conditioning Engineers Inc., Atlanta, 187-199, (2005).

Chiam, H. W., Azmi, W. H., Usri, N. A., Mamat, R. and Adam, N. M., Thermal conductivity and viscosity of Al_2O_3 nanofluids for different based ratio of water and ethylene glycol mixture, *Exp. Therm. Fluid Sci*., 81, 420–429 (2017). https://doi.org/10.1016/j.expthermflusci.2016.09.013

Choi, S. U. S. and Eastman J. A., Enhancing thermal conductivity of fluids with nanoparticles, *ASME International Mechanical Engineering Congress & Exposition,* 12-15, (1995).

Elsaid, K., Abdelkareem, M. A., Maghrabie, H. M., Sayed, E. T., Wilberforce, T., Baroutaji, A. and Olabi, A. G., Thermophysical properties of graphene-based nanofluids, *Int. J. Thermofluids*, 10, 100073 (2021). https://doi.org/10.1016/j.ijft.2021.100073

Hachey, M. A., Nguyen, C. T., Galanis, N. and Popa, C. V., Experimental investigation of Al2O3 nanofluids thermal properties and rheology - Effects of transient and steady-state heat exposure, *Int. J. Therm. Sci*., 76, 155–167 (2014). https://doi.org/10.1016/j.ijthermalsci.2013.09.002

Hummers, W. S. and Offeman, R. E., Preparation of graphitic oxide, *J. Am. Chem. Soc.,* 80(6), 1339 (1958). https://doi.org/10.1021/ja01539a017

Sundar, L. S., Singh, M. K. and Sousa, A. C. M., Enhanced thermal properties of nanodiamond nanofluids, *Chem. Phys. Lett.,* 644, 99–110 (2016a). https://doi.org/10.1016/j.cplett.2015.11.028

Jamei, M., Karbasi, M., Dehkordi, M. M., Olumegbon, I. A., Abualigah, L., Said, Z. and Asadi, A., Estimating the density of hybrid nanofluids for thermal energy application: Application of non-parametric and evolutionary polynomial regression data-intelligent techniques, *Meas.,* 189 110524 (2022). https://doi.org/10.1016/j.measurement.2021.110524

Liu, M.S., Lin, M. C. C. and Wang, C. C., Enhancements of thermal conductivities with Cu, CuO, and carbon nanotube nanofluids and application of MWNT/water nanofluid on a water chiller system, *Nanoscale Res Lett*., 6, 297 (2011). https://doi.org/10.1186/1556-276X-6-297

Montazer, E., Salami, E., Yarmand, H., Chowdhury, Z. Z., Dahari, M., Kazi, S. N. and Badarudin, A., Development of a new density correlation for carbon-based nanofluids using response surface methodology, *J. Therm. Anal. Calorim*., 132, 1399–1407 (2018). https://doi.org/10.1007/s10973-018-6978-4

Nguyen, C. T., Desgranges, F., Galanis, N., Roy, G., Mare, T., Boucher S. and Mintsa, A. H., Viscosity data for Al_2O_3-water nanofluid e hysteresis: is heat transfer enhancement using nanofluids reliable, *Int. J. Therm. Sci*., 47(2), 103–111 (2008). https://doi.org/10.1016/j.ijthermalsci.2007.01.033

Pathipakka, G. and Sivashanmugam, P., Heat transfer behaviour of nanofluids in a uniformly heated circular tube fitted with helical inserts in laminar flow, *Superlatt. Microstruct.,* 47(2), 349–360 (2010). https://doi.org/10.1016/j.spmi.2009.12.008

Radkar, R. N., Bhanvase, B. A., Barai, D. P. and Sonawane, S. H., Intensified convective heat transfer using ZnO nanofluids in heat exchanger with helical coiled geometry at constant wall temperature, *Mater. Sci. Energy Technol*., 2(2), 161–170 (2019). https://doi.org/10.1016/j.mset.2019.01.007

Satti, J. R., Das, D. K. and Ray, D., Specific heat measurements of five different propylene glycol based nanofluids and development of a new correlation, *Int. J. Heat Mass Transf*., 94, 343–353 (2016). https://doi.org/10.1016/j.ijheatmasstransfer.2015.11.065

Shahrul, I. M., Mahbubul, I. M., Khaleduzzaman, S. S., Saidur, R. and Sabri, M. F. M., A comparative review on the specific heat of nanofluids for energy perspective, *Renew. Sustain. Energy Rev.,* 38, 88–98 (2014). https://doi.org/10.1016/j.rser.2014.05.081

Srinivasan, D., Senthilkumar, N., Ganesh, M. and Perumal, G., Characterization studies on nano aluminium composite reinforced with montmorillonite nanoclay and titanium carbide, *Multiscale Multidiscip. Model. Exp. Des*., 7, 2839–2859 (2024). https://doi.org/10.1007/s41939-024-00374-x

Sundar, L. S., Specific heat analysis of water and ethylene glycol based rGO-ND hybrid nanofluids: Experimental and artificial neural network predictions, *J. Nano Res*., 86, 89-109 (2024). https://doi.org/10.4028/p-xEF4XO

Sundar, L. S., Naik, M. T., Sharma, K. V., Singh, M. K. and Reddy, S. C. T., Experimental investigation of forced convection heat transfer and friction factor in a tube with Fe3O4 magnetic nanofluid, *Exp. Therm. Fluid Sci.,* 37, 65–71 (2012). https://doi.org/10.1016/j.expthermflusci.2011.10.004

Sundar, L. S., Singh, M. K. and Sousa, A. C. M., Experimental thermal conductivity and viscosity of nanodiamond-based propylene glycol and water mixtures, *Diamond Relat. Mater.,* 69, 49-60 (2016b). https://doi.org/10.1016/j.diamond.2016.07.007

Vallarasu, K., Sampathkumar, V., Manoj, S., Raja, K., Vijayalakshmi, V., Gopalakrishnan, K. M. and Navaneethan, K. S., Catalytical Degradation of Industrial Dyes using Biosynthesized Nanoparticles – Review, *J. Environ. Nanotechnol.,* 12(4), 93-107(2023). https://doi.org/10.13074/jent.2023.12.234489

Vajjha, R. S., Das, D. K. and Mahagaonkar, B. M., Density measurement of different nanofluids and their comparison with theory, *Pet. Sci. Technol.,* 27(6), 612-624 (2006). https://doi.org/10.1080/10916460701857714

Yadav, D., Nirala, A., Kumar, R. and Singh, P. K., Density variation in nanofluids as a function of concentration and temperature, *Mater. Today: Proc*., 46, 6576-6580 (2021). https://doi.org/10.1016/j.matpr.2021.04.052

Yıldırımcan, S. Influence of antimony doping on structural, morphological and optical properties of CuO powders, *Adv. Eng. Sci*., 4, 120–129 (2024).

Zhelezny, V. P., Motovoy, I. V. and Ustyuzhanin, E. E., Prediction of nanofluids properties: the density and the heat capacity, *J. Phys.: Conf. Ser*., 891, 012347 (2017). https://doi.org/10.1088/1742-6596/891/1/012347

.